that can regulate these systems. The field of science on this is in its infancy.

REFERENCES AND NOTES

1. P. E. Converse, in *Ideology and Its Discontents*, D. E. Apter, Ed. (The Free Press of Glencoe, 1964), pp. 206–261.
2. E. H. Spicer, *Science* **174**, 795–800 (1971).
3. J.-B. Michel *et al.*, *Science* **331**, 176–182 (2011).
4. E. Griffiths, *Towards a Science of Belief Systems* (Palgrave Macmillan, 2014).
5. L. Festinger, *A Theory of Cognitive Dissonance* (Stanford Univ. Press, 1957).
6. B. Gawronski, F. Strack, Eds., *Cognitive Consistency: A Fundamental Principle in Social Cognition* (Guilford, 2012).
7. M. H. DeGroot, *J. Am. Stat. Assoc.* **69**, 118–121 (1974).
8. R. Axelrod, *J. Conflict Resolut.* **41**, 203–226 (1997).
9. N. E. Friedkin, *A Structural Theory of Social Influence* (Cambridge Univ. Press, 1998).
10. D. A. Snow, S. A. Soule, H. Kriesi, Eds., *The Blackwell Companion to Social Movements* (Blackwell, 2004).
11. V. Blondel, J. Hendrickx, J. Tsitsiklis, *IEEE Trans. Automat. Contr.* **54**, 2586–2597 (2009).
12. A. Flache, M. W. Macy, *J. Math. Sociol.* **35**, 146–176 (2011).
13. P. V. Marsden, Ed., *Social Trends in American Life: Findings from the General Social Survey Since 1972* (Princeton Univ. Press, 2012).
14. C. Altafini, *IEEE Trans. Automat. Contr.* **58**, 935–946 (2013).
15. N. E. Friedkin, E. C. Johnsen, *Social Influence Network Theory: A Sociological Examination of Small Group Dynamics* (Cambridge Univ. Press, 2011).
16. P. Frasca, H. Ishii, C. Ravazzi, R. Tempo, *Eur. J. Control* **24**, 2–13 (2015).
17. N. E. Friedkin, *IEEE Control Systems* **35**, 40–51 (2015).
18. S. E. Parsegov, A. V. Proskurnikov, R. Tempo, N. E. Friedkin, *IEEE Trans. Automat. Contr.* (2016); published online at http://ieeexplore.ieee.org/document/7577815/
19. www.gallup.com/poll/7303/public-iraq-fails-inspections-second-un-resolution-needed-war.aspx
20. www.gallup.com/poll/7408/public-taking-waitandsee-attitude-un-inspections.aspx
21. www.people-press.org/2003/01/16/public-wants-proof-of-iraqi-weapons-programs/
22. http://usatoday30.usatoday.com/news/world/iraq/2003-03-16-poll-iraq_x.htm
23. www.gallup.com/poll/7720/powells-un-appearance-important-public.aspx
24. www.washingtonpost.com/wp-srv/nation/transcripts/powelltext_020503.html
25. www.pewresearch.org/2008/03/19/public-attitudes-toward-the-war-in-iraq-20032008/
26. I. L. Janis, *Groupthink: Psychological Studies of Policy Decisions and Fiascoes* (Houghton Mifflin, 1982).

ACKNOWLEDGMENTS

N.E.F. acknowledges the financial support of the U.S. Army Research Laboratory and the U.S. Army Research Office under grant no. W911NF-15-1-0577. A.V.P. acknowledges Russian Science Foundation project 14-29-00142 hosted by IPME RAS, under whose financial support the results from section S2.3.2 were obtained. Partial financial support was also provided by European Research Council grant ERCStG-307207 hosted by the University of Groningen. R.T. acknowledges the financial support of the National Research Council of Italy. S.E.P. acknowledges the financial support of Russian Science Foundation project 16-11-00063 hosted by the V.A. Kotelnikov Institute of Radio Engineering and Electronics of the Russian Academy of Sciences.

SUPPLEMENTARY MATERIALS

www.sciencemag.org/content/354/6310/321/suppl/DC1
Supplementary Text
Fig. S1
References (*27*–*34*)

31 May 2016; accepted 7 September 2016
10.1126/science.aag2624

PLANKTON DYNAMICS

Physiological and ecological drivers of early spring blooms of a coastal phytoplankter

Kristen R. Hunter-Cevera,[1] Michael G. Neubert,[1] Robert J. Olson,[1] Andrew R. Solow,[2] Alexi Shalapyonok,[1] Heidi M. Sosik[1]*

Climate affects the timing and magnitude of phytoplankton blooms that fuel marine food webs and influence global biogeochemical cycles. Changes in bloom timing have been detected in some cases, but the underlying mechanisms remain elusive, contributing to uncertainty in long-term predictions of climate change impacts. Here we describe a 13-year hourly time series from the New England shelf of data on the coastal phytoplankter *Synechococcus*, during which the timing of its spring bloom varied by 4 weeks. We show that multiyear trends are due to temperature-induced changes in cell division rate, with earlier blooms driven by warmer spring water temperatures. *Synechococcus* loss rates shift in tandem with division rates, suggesting a balance between growth and loss that has persisted despite phenological shifts and environmental change.

Marine phytoplankton account for one-half of global primary production. Of considerable interest and concern is how climate change may affect this production. Increased temperature, ocean acidification, and altered nutrient delivery all have the potential to affect phytoplankton dynamics, including the timing and magnitude of blooms, which can dominate seasonal productivity (*1*, *2*). There is evidence of current and ongoing changes in plankton phenology (*3*–*5*), with potentially substantial ecological consequences for marine systems (*6*).

Recently, there has been uncertainty about the detection of trends in phytoplankton biomass and how possible trends relate to climate change (*7*–*9*). The uncertainty arises in part from difficulties in species-level detection of phytoplankton. Many studies use bulk measurements that reflect a composite of the phytoplankton community (*10*). These measurements (such as chlorophyll concentration) can mask taxon-specific changes and obscure the mechanisms that govern responses to climate change. Another challenge lies in the need to observe and measure phytoplankton at appropriate time scales to elucidate those mechanisms. Ecological interactions and physiological responses of phytoplankton are rapid (on the order of minutes to hours). To adequately capture population dynamics, we must sample at this frequency, but also for extended durations because identification of seasonal, yearly, or decadal trends requires time series of these lengths.

We address this lack of temporal and taxonomic resolution for the picophytoplankter *Synechococcus* by using observations of individual cells and their properties from an automated submersible flow cytometer, FlowCytobot (FCB) (*11*) , deployed at the Martha's Vineyard Coastal Observatory (MVCO). FCB has been deployed at MVCO since 2003, with year-round observations beginning in 2007. The data consist of a 13-year time series of hourly measurements of *Synechococcus* concentration and cell properties.

At MVCO, *Synechococcus* concentration exhibits a strong seasonal cycle, with low concentrations in winter and early spring, followed by a two- to three-order-of-magnitude bloom event in late spring (Fig. 1A). The population fluctuates around a slowly declining trend during summer and early fall and then declines sharply in late fall. Although this classic pattern (*12*) is stable from year to year, we found that the timing of the spring bloom varied by up to 4 weeks within our time series, and in particular we noted a trend of earlier blooms from 2003 to 2012 (~20-day advance) and later blooms from 2013 to 2015. We quantified these shifts by determining the day of the year at which the concentration first exceeds threshold concentration levels (Fig. 2B and fig. S1). Concurrent observations of temperature (Fig. 1D) show that earlier blooms coincide with warmer spring conditions (Fig. 2A and fig. S2). For each degree increase of the mean temperature in April, the spring bloom advances 4 to 5 days. The water at MVCO has been warming (fig. S3) in a manner consistent with the multidecadal trend in this region (*13*). Large seasonal and interannual variations are superimposed on these warming trends.

Numerous studies have identified correlations between temperature and *Synechococcus* concentration across a range of ocean conditions (*12*, *14*–*17*). In particular, there is evidence that the spring bloom begins in northeast U.S. and Canadian waters when the temperature exceeds

[1]Biology Department, Woods Hole Oceanographic Institution, Woods Hole, MA 02543, USA. [2]Marine Policy Center, Woods Hole Oceanographic Institution, Woods Hole, MA 02543, USA.
***Corresponding author. Email: hsosik@whoi.edu**

~6°C (*12*, *18*). In addition, studies with cultured isolates have shown that *Synechococcus* physiology is temperature-dependent (*19*, *20*). However, in situ evidence of a direct link between cell division rates and temperature is limited (*12*, *19*, *20*).

To understand the mechanism underlying the phenology shifts at MVCO, it is necessary to separate contributions from cell division and cell loss. Traditional methods for doing so require labor-intensive measurements (*21*, *22*) that are impractical to sustain over months and years. Instead, we used a method that exploits the diel variations in the cell size of *Synechococcus* (*17*) (fig. S4). Cells typically increase in volume during daylight hours as they photosynthesize and then decrease in volume in the evening through cell division. By fitting a matrix population model to the size-distribution time series, it is possible to accurately estimate daily population division rates for *Synechococcus* (*17*). The same method also works well for other phytoplankton

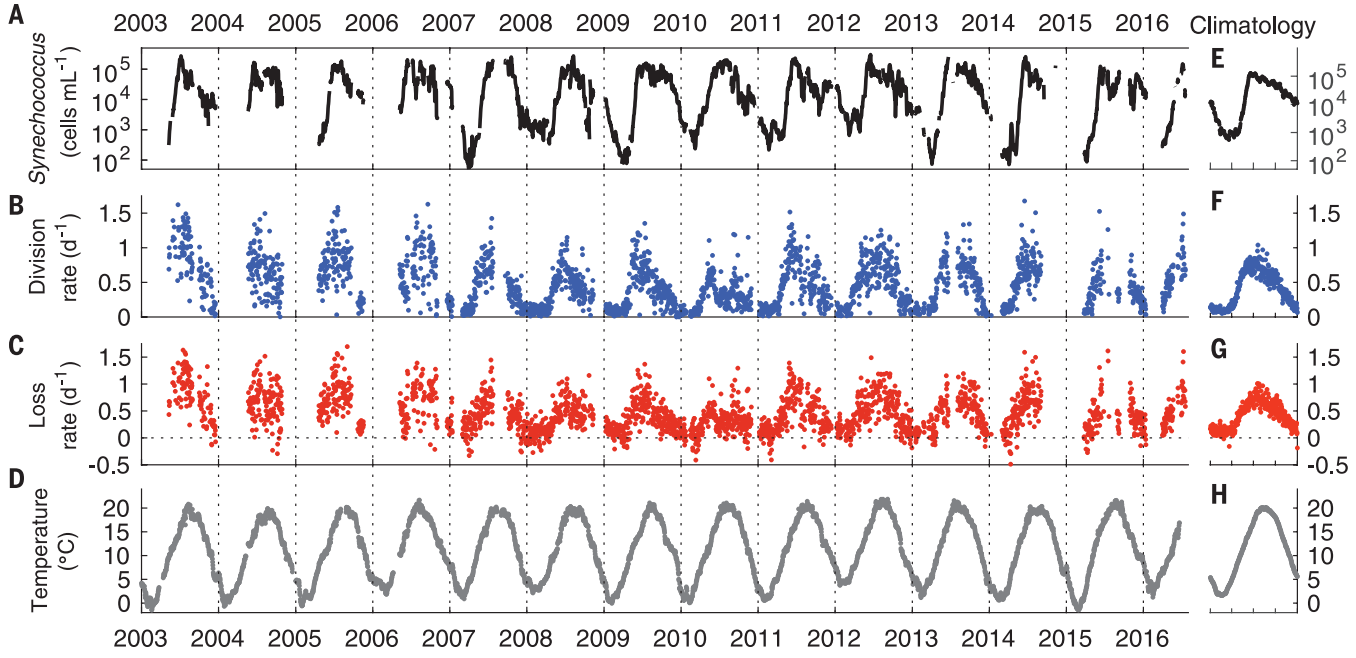

Fig. 1. Daily time series at MVCO from 2003 to 2016. (**A**) Averaged *Synechococcus* cell concentration (cells per milliliter). (**B**) Division rates estimated with a matrix population model [per day (d)]. (**C**) Loss rates calculated by subtracting net growth rate [obtained from changes in (A)] from division rate (B). (**D**) Water temperature (degrees Celsius). Climatology (mean annual pattern for the time series) is shown on the right for (**E**) *Synechococcus* cell concentration, (**F**) division rate, (**G**) loss rate, and (**H**) water temperature.

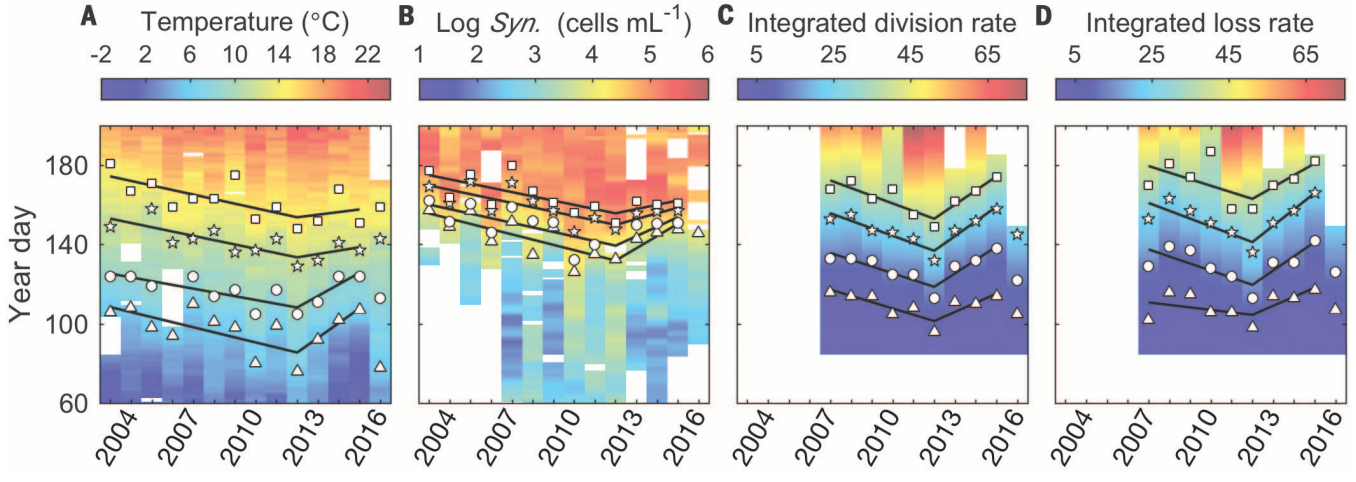

Fig. 2. Multiyear trends showing spring temperature changes and *Synechococcus* bloom shifts from 2003 to 2016. The data are shown by day of the year (vertical axis), with values denoted by color. (**A**) Temperature. Markers indicate the day in each year when water temperature first exceeds 6° (triangles), 9° (circles), 12° (stars), or 15°C (squares). (**B**) *Synechococcus* cell concentration. Markers indicate the day in each year when cell concentration exceeds 8×10^3 (triangles), 1.6×10^4 (circles), 4.8×10^4 (stars), or 9.6×10^4 (squares) cells ml^{-1}. (**C**) Integrated division rate (cumulative summed division rate starting at year day 85). Markers indicate the day in each year when the integrated division rate exceeds values of 4 (triangles), 12 (circles), 24 (stars) or 36 (squares). (**D**) Integrated loss rate (cumulative summed loss rate starting at year day 85). Markers indicate the day in each year when the integrated loss rate exceeds values of 4 (triangles), 12 (circles), 24 (stars), or 36 (squares). Solid lines in each panel represent best fits from a piecewise linear regression model between year-day threshold crossings (as denoted by the markers) and year. Parallel lines reflect insensitivity to the choice of threshold and a shift in only the timing, not in the shape, of the spring bloom trajectory.

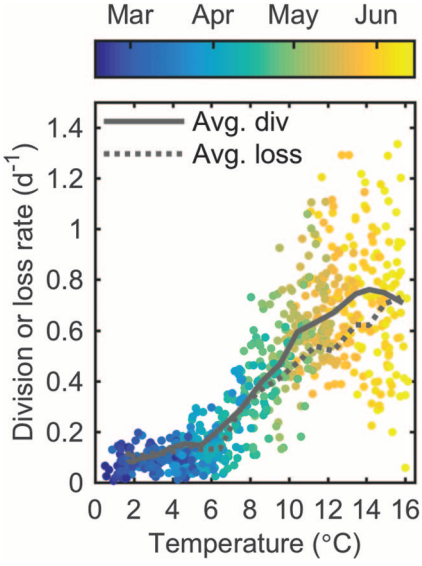

Fig. 3. Relationship between division rates and temperature between 1 February and 15 June for all data points (2003–2016). Colors indicate day of the year. The solid line is the relationship between the weekly climatology of division rate and the weekly climatology of temperature. The dashed line is the relationship between the weekly climatology of loss rate and the weekly climatology of temperature.

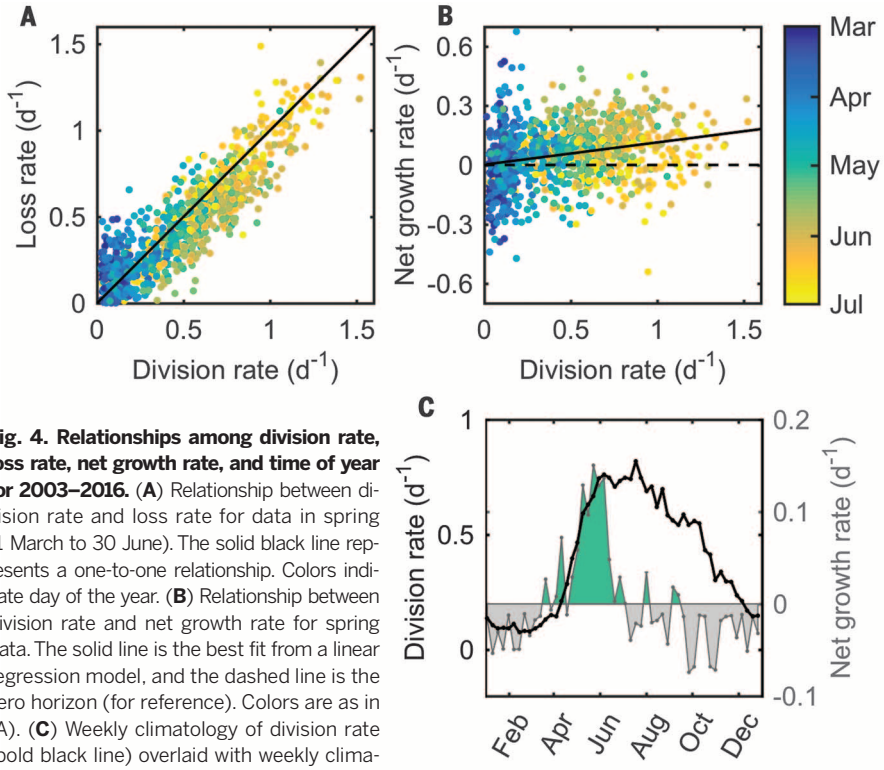

Fig. 4. Relationships among division rate, loss rate, net growth rate, and time of year for 2003–2016. (**A**) Relationship between division rate and loss rate for data in spring (1 March to 30 June). The solid black line represents a one-to-one relationship. Colors indicate day of the year. (**B**) Relationship between division rate and net growth rate for spring data. The solid line is the best fit from a linear regression model, and the dashed line is the zero horizon (for reference). Colors are as in (A). (**C**) Weekly climatology of division rate (bold black line) overlaid with weekly climatology of net growth rate (thin gray line). Periods of positive (negative) net growth rate are indicated with green (gray) shading.

species (*23*, *24*). The model relies only on changes in cell size and not on changes in cell concentration, which are often decoupled from division rate (fig. S4) as a result of cell loss or advection. Isolating the contribution of cell division is critical, because the net population growth rate is typically much lower than the division rate as a result of the tight coupling between primary producers and consumers in planktonic ecosystems (*25*). In combination with sustained, high-resolution in situ observations, this model makes it possible to produce the multiyear records of daily division rate (Fig. 1B) that are required to understand phenological shifts.

Model-estimated division rates reflect a composite response of the entire *Synechococcus* population. Natural populations are often composed of more than one *Synechococcus* type, and multiple genotypes are known to coexist at MVCO (*26*, *27*). Types can differ in physiological characteristics, such as temperature growth response or tolerance (*20*). Nonetheless, we find that *Synechococcus* division rates exhibit a pronounced seasonality, suggesting strong environmental drivers for the entire population. The division rate is as low as 0.1 day^{-1} in winter and as high as 1.4 day^{-1} in spring (Fig. 1B), increasing rapidly after water temperature exceeds ~5°C (Fig. 3). The increase slows or stops once water temperature reaches ~16°C in spring. The shape of the relationship between temperature and division rate strongly resembles that of the relationship for cultured *Synechococcus* (*19*, *20*). During spring, a single clade-I genotype makes up the majority of the population (*26*). A cultured MVCO isolate belonging to this clade exhibits the same relationship between division rate and temperature as we report here for the natural population (*17*) (fig. S5). No other environmental factor (light or nutrients) shows such a strong relationship with in situ division rate in spring (fig. S6). Together, these results support the view that temperature is the main factor limiting *Synechococcus* division during late winter and spring (*17*).

Our second main result is that the phenological shifts of the spring bloom are caused by temperature-induced shifts in the timing of the division rate increase (fig. S2). Specifically, the date at which population growth potential (computed as the integrated division rate for each day in spring; methods and fig. S7) reached threshold values advanced over the warming period 2003–2012 but retreated when spring temperatures cooled in 2013–2015 (Fig. 2C). The record-warm conditions in 2012 mark a transition between periods of advancing and retreating that are coincident across threshold crossings for spring temperature, *Synechococcus* concentration, and integrated division rate. In conjunction with the temperature dependence of the division rate in spring (Fig. 3), this result supports the conclusion that shifts in the timing of spring blooms reflect a direct physiological response to shifts in the onset of seasonal warming.

If division rates were the only factor affecting bloom phenology, we would expect not only a shift in timing, but also a change in the rate of increase in cell concentration. In fact, only the timing has shifted, whereas the rate of increase in cell concentration has not changed systematically (Fig. 2B). The stability of the bloom trajectory suggests that population losses have also shifted in tandem with growth (Fig. 2D and fig. S7). To illustrate this, we calculated bulk *Synechococcus* loss rates by subtracting the division rate from the net growth rate. The loss rates closely track division rates in magnitude over the entire time series (Fig. 1C), but during the spring bloom, the loss rate is on average ~ 0.15 day^{-1} lower than the division rate (Fig. 4A). It is this slight imbalance persisting for several months that leads to a steady blooming phase. The narrow margin by which *Synechococcus* can essentially "outgrow" their losses in spring makes this a critical time for cells to accumulate.

Our third main result, that loss rates closely track division rates, suggests that the dominant losses are biological (e.g., viral lysis and grazing) rather than physical in nature. It is unlikely that advection of spatial patches, for instance, would produce this tight correspondence year after year.

Beyond the connection to climate, our findings provide important insights into the ways that physiology and environmental factors interact to control phytoplankton blooms, a classic problem that has been the subject of recent controversy (*28*). Considering bulk properties of phytoplankton, Behrenfeld and Boss (*29*) have recently argued that, despite decades of study, no evidence has emerged linking bloom dynamics to physiological factors that regulate phytoplankton division rates. This led them to conclude that

bloom dynamics depend principally on the impact of consumers, a long-recognized control of phytoplankton abundance (*30*). Our findings for *Synechococcus* agree with those of Behrenfeld and Boss in so far as division rates (and, by inference, loss rates) are roughly 10 times the accumulation (net growth) rates. Our results differ, however, in that we find a significant positive correlation between division and accumulation rates over the course of the spring bloom (Fig. 4, B and C). This correlation was not detected by Behrenfeld and Boss, and perhaps should not be expected to be evident in the satellite-based observations of chlorophyll concentration that they analyzed (*29*). Those observations aggregate the entire phytoplankton community over a relatively large region of the ocean and mask individual responses of different taxa.

Our observations, made at a much smaller spatial scale and with much finer taxonomic and temporal resolution than that of satellite data, reveal a connection between division rates and the bloom dynamics of *Synechococcus*. Consumers (including grazers, viruses, and parasites) certainly play a major role in shaping the bloom's trajectory, but the bloom is triggered by an environmental factor, the seasonal temperature rise, which leads to increases in the *Synechococcus* division rate (Fig. 3). The bloom persists until the division rate plateaus (Fig. 4B), at which point losses overtake division and the bloom begins to decline.

We were able to diagnose the importance of temperature in regulating the dynamics of a ubiquitous marine primary producer, *Synechococcus,* by exploiting a 13-year time series comprising data on millions of individual cells and their traits. This allowed us to not only quantify the relationship between temperature and cell division in a natural population, but also to document how that relationship is the basis for a dramatic phenological shift affecting both *Synechococcus* and their consumers. It remains to be seen whether this ecological coupling will hold as warming trends continue in the decades to come.

REFERENCES AND NOTES

1. K. R. Arrigo, D. Worthen, A. Schnell, M. P. Lizotte, *J. Geophys. Res. Oceans* **103**, 15587–15600 (1998).
2. P. Martin *et al.*, *Deep Sea Res. Part I Oceanogr. Res. Pap.* **58**, 338–349 (2011).
3. R. Ji, M. Edwards, D. L. Mackas, J. A. Runge, A. C. Thomas, *J. Plankton Res.* **32**, 1355–1368 (2010).
4. K. H. Wiltshire *et al.*, *Estuaries Coasts* **33**, 295–310 (2010).
5. M. Kahru, V. Brotas, M. Manzano-Sarabia, B. G. Mitchell, *Glob. Change Biol.* **17**, 1733–1739 (2011).
6. M. Edwards, A. J. Richardson, *Nature* **430**, 881–884 (2004).
7. A. McQuatters-Gollop *et al.*, *Nature* **472**, E6–E7, discussion E8–E9 (2011).
8. W. W. Gregg, C. S. Rousseaux, *J. Geophys. Res. Oceans* **119**, 5921–5933 (2014).
9. D. G. Boyce, M. Dowd, M. R. Lewis, B. Worm, *Prog. Oceanogr.* **122**, 163–173 (2014).
10. D. A. Siegel *et al.*, *Remote Sens. Environ.* **135**, 77–91 (2013).
11. R. J. Olson, A. A. Shalapyonok, H. M. Sosik, *Deep Sea Res. Part I Oceanogr. Res. Pap.* **50**, 301–315 (2003).
12. J. B. Waterbury, S. W. Watson, F. W. Valois, D. G. Franks, *Can. Bull. Fish. Aquat. Sci.* **214**, 71–120 (1986).
13. S. W. Nixon, S. Granger, B. A. Buckley, M. Lamont, B. Rowell, *Estuaries* **27**, 397–404 (2004).
14. N. S. R. Agawin, C. M. Duarte, S. Agusti, *Mar. Ecol. Prog. Ser.* **170**, 45–53 (1998).
15. W. K. W. Li, *Limnol. Oceanogr.* **43**, 1746–1753 (1998).
16. A.-Y. Tsai, K.-P. Chiang, J. Chang, G.-C. Gong, *Aquat. Microb. Ecol.* **51**, 263–274 (2008).
17. K. R. Hunter-Cevera *et al.*, *Proc. Natl. Acad. Sci. U.S.A.* **111**, 9852–9857 (2014).
18. W. K. W. Li, W. G. Harrison, E. J. H. Head, *Proc. R. Soc. London Ser. B* **273**, 1953–1960 (2006).
19. L. R. Moore, R. Goericke, S. W. Chisholm, *Mar. Ecol. Prog. Ser.* **116**, 259–275 (1995).
20. J. Pittera *et al.*, *ISME J.* **8**, 1221–1236 (2014).
21. M. R. Landry, R. P. Hassett, *Mar. Biol.* **67**, 283–288 (1982).
22. R. E. McDuff, S. W. Chisholm, *Limnol. Oceanogr.* **27**, 783–788 (1982).
23. M. Dugenne *et al.*, *Front. Microbiol.* **5**, 485 (2014).
24. F. Ribalet *et al.*, *Proc. Natl. Acad. Sci. U.S.A.* **112**, 8008–8012 (2015).
25. A. Calbet, M. R. Landry, *Limnol. Oceanogr.* **49**, 51–57 (2004).
26. K. R. Hunter-Cevera, thesis, Massachusetts Institute of Technology and Woods Hole Oceanographic Institution (2014).
27. K. R. Hunter-Cevera, A. F. Post, E. E. Peacock, H. M. Sosik, *Microb. Ecol.* **71**, 276–289 (2016).
28. A. Fischer *et al.*, *Oceanography* **27**, 222–235 (2014).
29. M. J. Behrenfeld, E. S. Boss, *Annu. Rev. Mar. Sci.* **6**, 167–194 (2014).
30. K. Banse, in *Primary Productivity and Biogeochemical Cycles in the Sea*, P. G. Falkowski, A. D. Woodhead, K. Vivirito, Eds. (Springer, 1992), pp. 409–440.

ACKNOWLEDGMENTS

We thank E. T. Crockford, E. Peacock, J. Fredericks, the MVCO Operations Team, the captain and mate of the R/V *Tioga*, and P. Henderson of the Woods Hole Oceanographic Institution (WHOI) Nutrient Analytical Facility for logistical and analytical support. We thank S. W. Chisholm and J. Waterbury for discussions and comments on the manuscript. This work was supported by U.S. NSF grants OCE-0119915, OCE-0530830, OCE-1031256, DEB-1145017, and DEB-1257545; NASA grants NNX11AF07G and NNX13AC98G; Gordon and Betty Moore Foundation grant GGA#934; the Investment in Science Fund, given primarily by WHOI Trustee and Corporation Members; and a National Defense Science and Engineering graduate fellowship from the U.S. Department of Defense. Data used in this study were deposited in the Dryad Digital Repository (http://dx.doi.org/10.5061/dryad.jm8s7).

SUPPLEMENTARY MATERIALS

www.sciencemag.org/content/354/6310/326/suppl/DC1
Materials and Methods
Figs. S1 to S8
References (*31*–*33*)

10 April 2016; accepted 9 September 2016
10.1126/science.aaf8536

BIOMASS PROCESSING

Formaldehyde stabilization facilitates lignin monomer production during biomass depolymerization

Li Shuai,[1] Masoud Talebi Amiri,[1] Ydna M. Questell-Santiago,[1] Florent Héroguel,[1] Yanding Li,[2,3] Hoon Kim,[2,4] Richard Meilan,[5] Clint Chapple,[6] John Ralph,[2,3,4] Jeremy S. Luterbacher[1]*

Practical, high-yield lignin depolymerization methods could greatly increase biorefinery productivity and profitability. However, development of these methods is limited by the presence of interunit carbon-carbon bonds within native lignin, and further by formation of such linkages during lignin extraction. We report that adding formaldehyde during biomass pretreatment produces a soluble lignin fraction that can be converted to guaiacyl and syringyl monomers at near theoretical yields during subsequent hydrogenolysis (47 mole % of Klason lignin for beech and 78 mole % for a high-syringyl transgenic poplar). These yields were three to seven times those obtained without formaldehyde, which prevented lignin condensation by forming 1,3-dioxane structures with lignin side-chain hydroxyl groups. By depolymerizing cellulose, hemicelluloses, and lignin separately, monomer yields were between 76 and 90 mole % for these three major biomass fractions.

Lignin is an abundant natural polymer, accounting for 15 to 30 weight % (wt %) of lignocellulosic biomass (*1*, *2*). Unlike cellulose and hemicellulosic polysaccharides, the other major constituents of biomass, lignin primarily consists of methoxylated phenylpropanoid (guaiacyl and syringyl) subunits. This structure gives lignin an energy density 30% greater than that of polysaccharide polymers and makes it one of the few natural large-scale sources of aromatic compounds (*3*, *4*). These properties make lignin-derived monomers useful precursors for renewable aromatic chemicals and drop-in fuels (*3*, *4*).

The longstanding interest in lignin valorization has translated into few commercial processes because of the lack of practical high-yield lignin depolymerization methods that can be used while upgrading biomass polysaccharides. Promising biorefinery fractionation or pretreatment processes—such as those using water (*5*), alcohol (*6*), tetrahydrofuran (THF) (*7*), ionic liquids (IL) (*8*), and γ-valerolactone (GVL) (*9*, *10*)—use high temperatures and/or inexpensive mineral acids (such as H_2SO_4 and HCl) that facilitate the removal of lignin and hemicelluloses (*5*, *11*). A large-scale source of lignin could likely come from a process using these technologies (*4*). However, the

Physiological and ecological drivers of early spring blooms of a coastal phytoplankter

Kristen R. Hunter-Cevera, Michael G. Neubert, Robert J. Olson, Andrew R. Solow, Alexi Shalapyonok and Heidi M. Sosik

Science **354** (6310), 326-329.
DOI: 10.1126/science.aaf8536

Drivers of phytoplankton blooms

Despite decades of study, there is little evidence to link increases in phytoplankton growth in response to springtime warming with the dynamics of phytoplankton blooms. This lack of understanding makes it difficult to make predictions about global biogeochemical cycling in response to climate change. Hunter-Cevera *et al.* analyzed over a decade of data collected hourly from the New England shelf between 2003 and 2016 (see the Perspective by Worden and Wilken). Blooms now occur 20 days earlier than at the start of observations, because earlier springtime warming stimulates cell division earlier each year. Nevertheless, despite the shift in timing, predatory organisms in the food chain are still ready to consume the superabundance, which brings the blooms to an abrupt end each year.

Science, this issue p. 326; see also p. 287